ISSN 1674-1056
http://cpb.iphy.ac.cn
http://iopscience.iop.org/cpb
中国物理 B
Chinese Physics
中国物理 Chinese Physics B

Ab initio investigation of excited state dual hydrogen bonding interactions and proton transfer mechanism for novel oxazoline compound

Yu-Sheng Wang(王玉生)[1], Min Jia(贾敏)[1], Qiao-Li Zhang(张巧丽)[1], Xiao-Yan Song(宋晓燕)[1], Da-Peng Yang(杨大鹏)[1,2]
Citation: Chin. Phys. B . 2019, 28(10): 103105 . **doi:** 10.1088/1674-1056/ab4042
Journal homepage: http://cpb.iphy.ac.cn; http://iopscience.iop.org/cpb

What follows is a list of articles you may be interested in

The substituent effect on the excited state intramolecular proton transfer of 3-hydroxychromone

Yuzhi Song(宋玉志), Songsong Liu(刘松松), Jiajun Lu(陆佳骏), Hui Zhang(张慧), Changzhe Zhang(张常哲), Jun Du(杜军)
Chin. Phys. B . 2019, 28(9): 093102 . **doi:** 10.1088/1674-1056/ab3434

Tensile-strain induced phonon splitting in diamond

Meifang Pu(蒲梅芳), Feng Zhang(张峰), Shan Liu(刘珊), Tetsuo Irifune(入舩徹男), Li Lei(雷力)
Chin. Phys. B . 2019, 28(5): 053102 . **doi:** 10.1088/1674-1056/28/5/053102

Accurate double many-body expansion potential energy surface of $HS_2(A^2A')$ by scaling the external correlation

Lu-Lu Zhang(张路路), Yu-Zhi Song(宋玉志), Shou-Bao Gao(高守宝), Yuan Zhang(张媛), Qing-Tian Meng(孟庆田)
Chin. Phys. B . 2016, 25(5): 053101 . **doi:** 10.1088/1674-1056/25/5/053101

Globally accurate *ab initio* based potential energy surface of $H_2O^+(X^4A'')$

Song Yu-Zhi, Zhang Yuan, Zhang Lu-Lu, Gao Shou-Bao, Meng Qing-Tian
Chin. Phys. B . 2015, 24(6): 063101 . **doi:** 10.1088/1674-1056/24/6/063101

A full-dimensional analytical potential energy surface for the $F+CH_4 \rightarrow HF+CH_3$ reaction

Yang Chuan-Lu, Wang Mei-Shan, Liu Wen-Wang, Zhang Zhi-Hong, Ma Xiao-Guang
Chin. Phys. B . 2013, 22(6): 063102 . **doi:** 10.1088/1674-1056/22/6/063102

Ab initio investigation of excited state dual hydrogen bonding interactions and proton transfer mechanism for novel oxazoline compound*

Yu-Sheng Wang(王玉生)[1,†], Min Jia(贾敏)[1], Qiao-Li Zhang(张巧丽)[1], Xiao-Yan Song(宋晓燕)[1], and Da-Peng Yang(杨大鹏)[1,2]

[1] College of Physics and Electronics, North China University of Water Resources and Electric Power, Zhengzhou 450046, China
[2] State Key Laboratory of Molecular Reaction Dynamics, Dalian Institute of Chemical Physics, Chinese Academy of Sciences, Dalian 116023, China

(Received 7 June 2019; revised manuscript received 24 August 2019; published online 30 September 2019)

Owing to the importance of excited state dynamical relaxation, the excited state intramolecular proton transfer (ESIPT) mechanism for a novel compound containing dual hydrogen bond (abbreviated as "1-enol") is studied in this work. Using density functional theory (DFT) and time-dependent density functional theory (TDDFT) method, the experimental electronic spectra can be reproduced for 1-enol compound. We first verify the formation of dual intramolecular hydrogen bonds, and then confirm that the dual hydrogen bond should be strengthened in the first excited state. The photo-excitation process is analyzed by using frontier molecular orbital (HOMO and LUMO) for 1-enol compound. The obvious intramolecular charge transfer (ICT) provides the driving force to effectively facilitate the ESIPT process in the S_1 state. Exploration of the constructed S_0-state and S_1-state potential energy surface (PES) reveals that only the excited state intramolecular single proton transfer occurs for 1-enol system, which makes up for the deficiencies in previous experiment.

Keywords: excited state intramolecular proton transfer, potential energy surface, intramolecular charge transfer, infrared vibrational spectra

PACS: 31.15.ee, 31.15.ae, 31.15.es **DOI:** 10.1088/1674-1056/ab4042

1. Introduction

As one of the most fundamental non-covalent weak interactions, hydrogen bond exists anywhere in our natural life. In the past few decades, more and more researches have been devoted to investigating the hydrogen bonding interactions.[1–3] In fact, hydrogen bond can be represented in the X–H$\cdots Y$ form, where X and Y denote the atoms having high electronegativity and small radius, such as O, N, F or the like. When the hydrogen atom forms a covalent bond with the electronegative atom, the shared electronic pair is biased towards another electronegative atom. That should be the simple explanation for the formation of hydrogen bond.[1–3] Among the various chemical reactions, the proton transfer (PT) is a characteristic process in chemical and biological acid-based neutralization reactions. Based on the excitation of light, the initial hydrogen bonding intensity makes a difference, which becomes favorable for the excited state intramolecular proton transfer (ESIPT) process.[4–9] Since Weller first reported ESIPT in the middle of the last century,[10] this kind of chemical reaction has attracted lots of attention. Since Han and coworkers put forward a novel excited state hydrogen bonding strengthening mechanism,[11–16] the dynamical behaviors about excited state hydrogen bonding interactions have been strongly attractive. Essentially, the ESIPT mechanism has become a hot research topic in excited state relaxations currently. Particularly, the rapid charge recombination and unique dual emission phenomenon endow ESIPT compounds with extensive applications, such as molecular switches, laser dyes, fluorescence chemosensors, UV filters, *etc*.[17–28]

It cannot be denied that most of chemical and biological systems exhibit multiple hydrogen bonding interactions. Therefore, the case about ESIPT process involved in single hydrogen bonding wire is not enough to imitate the biological behaviors. Therefore, to further explore the excited state behaviors along with multiple hydrogen bonds, one pays attention to the excited state single or double proton transfer reaction along with double hydrogen bonds since this kind of case should be the most fundamental way to further investigate multiple proton behavior in future.[29–35] For example, Krishnamoorthy *et al.* theoretically explored the double excited state intramolecular proton transfer behavior for the novel 3,5-bis(2-hydroxyphenyl)-1 H-1,2,4-triazole (bis-HPTA).[29] The new type of sequential proton transfer is referred to as proton transfer triggered proton transfer mechanism.[29] Tang *et al.* elaborated the intramolecular proton relay behaviors and confirm the undergoing ESDPT reaction process.[30] Song *et al.* compared the intermolecular dual hydrogen bonding effects for

*Project supported by the National Natural Science Foundation of China (Grant No. 11404112), the Funding Scheme for Young Teachers in Colleges and Universities in Henan Province, China (Grant No. 2017GGJS077), and the Key Scientific Research Project of Colleges and Universities of Henan Province, China (Grant No. 18A140023).

†Corresponding author. E-mail: yswang7106@163.com

© 2019 Chinese Physical Society and IOP Publishing Ltd

3-hydroxyisoquinoline dimer and acidity compound.[31] They clearly clarified the detailed intermolecular dual PT behaviors. In addition, as a classical chemical system, 7-azaindole dimer has been explored by Crepo-Otero *et al.* in detail.[32] According to their simulated results, Crepo-Otero *et al.* presented that the stepwise mechanism is not consistent with the topography of the excited state.[32] As a whole, the investigation about ESPT reaction along with multiple hydrogen bonds is very important,[33–35] which plays a role in helping researchers to gain a more in-depth understanding of multiple proton behaviors in excited state.

Very recently, Reis *et al.* designed and synthesized a novel intramolecular dual hydrogen bond compound dimethyl-2,2'-(3,3"-dihydroxy-[1,1',4",1"-terphenyl]-4,4"-diyl)(4 S,4'S,5 S,5'S)-bis(5-methyl-4,5-dihydrooxazole-4-carboxylate) (abbreviated as "1-enol" according to Ref. [36], based on which the excited state dynamical process of this molecule has been explored. Experimentally, they measured the steady-state absorption and emission spectra in different solvents, and confirmed the ESIPT behavior of 1-enol compound via the dual emission peaks. They attributed the behaviors of first excited state to the double ESIPT reaction. Even though some simple simulations have been carried out, the solvent effects were not considered in the theoretical process.[36] In fact, direct information about the geometrical relaxation upon the photoexcitation and the transition state geometry is difficult to obtain from the experimental spectroscopic manners.[37–42] And it is worth mentioning that the ab initio excited state calculations can provide the missing information and in-depth insight into the mechanism of clear excited state behaviors. And it cannot be denied that none of some suggested mechanisms in experiment is usually completely correct and sometimes they are problematic.[43–49] Therefore, further theoretical study for validating the mechanism could provide guidance for developing novel ESIPT compounds.

In this present work, therefore, we mainly pay attention to the excited state dynamic behavior for 1-enol compound by using theoretical simulation manner. We show the corresponding structures for 1-enol compound in Fig. 1. Here in this paper, 1-spt and 1-dpt denote the single proton-transfer 1-enol and the double proton-transfer 1-enol forms, respectively. According to the density functional theory (DFT) and time-dependent density functional theory (TDDFT) method, we comprehend the detailed mechanism and clarify the fundamental aspects concerning the different electronic states and structures involved in the ESIPT reaction. Particularly, we clarify that the excited state intramolecular single proton transfer (ESISPT) mechanism rather than the double ESIPT process contributes to the 1-enol system.

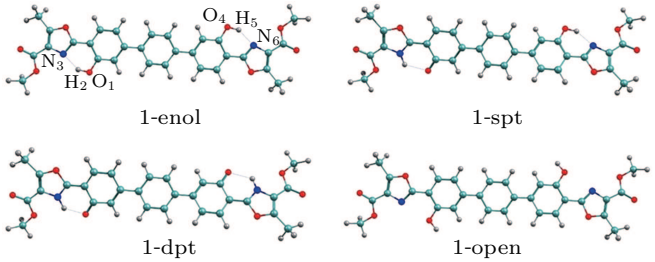


Fig. 1. Relative structures for 1-enol, 1-spt, 1-dpt, and their non-hydrogen bonding 1-open forms, where dual intramolecular hydrogen bonds are referred to as O_1–$H_2\cdots N_3$ and O_4–$H_5\cdots N_6$ for 1-enol configuration, respectively.

2. Theoretical methods

In this work, all calculations about structures and the stable energy for 1-enol system and its tautomers have been performed by using Gaussian 09 program.[50] And according to the DFT and TDDFT method with the Becke's three-parameter hybrid exchange function combined with the Lee–Yang–Parr gradient-corrected correlation functional (B3LYP) as well as the triple-ζ valence quality with one set of polarization functions (TZVP) basis set,[51–54] we perform the quantum chemical simulations. To consider the solvent effect (DMSO) adopted in previous experiment,[36] in this work, we select the integral equation formalism version of the polarizable continuum model (IEFPCM).[55,56] The ground state structures for all the structures involved in this work are optimized by using the DFT method, and the vibrational frequencies at the optimized structures are calculated by using the same DFT method to verify that the optimized configurations correspond to the local minima on the S_0-state potential energy surface (PES). Then, the photo-excitation process and corresponding charge redistribution are calculated by using the TDDFT method based on the optimized S_0-state 1-enol structure. The first singlet excited state of each tautomers is relaxed by using the TDDFT method to obtain its minimum energy geometry. The frequency calculations of selected excited state minima are also calculated to verify that they correspond to the local minima on the S_1-state PES. No constraints are imposed on symmetry, bond length, bond angle and dihedral angle in the simulation of geometry optimization. The PES of S_0 state and the PES of S_1 state are constructed each as a function of hydroxide radical length in a range from 0.9 Å to 2.1 Å in steps of 0.1 Å based on DFT and TDDFT method coupling with B3LYP/TZVP level in DMSO solvent, respectively.

The self-consistent field (SCF) convergence threshold of energy for each of S_0- and S_1-state optimizations is set to be 10^{-8} (default setting is 10^{-6}). The harmonic vibrational frequencies of S_0 and S_1 states are determined by the diagonalization of Hessian matrix. Excited-state Hessian matrix can be obtained by numerical differentiation of the analytical gradients via central differences and default displacements of 0.02

Bohr. And the infrared intensities are determined by the gradients of the dipole moment.

3. Results and discussion

The 1-enol possesses dual intramolecular hydrogen bonds and a symmetrical structure. Therefore, we can locate three kinds of structures (*i.e.*, 1-enol itself, its single proton-transfer 1-spt form, and its double-proton transfer 1-dpt form) in S_0 and S_1 states (Fig. 1). For convenience, we name the dual intramolecular hydrogen bonds O_1–$H_2\cdots N_3$ and O_4–$H_5\cdots N_6$ for 1-enol system, respectively. In the process of investigating the possible correlation of the electronic potential with hydrogen bonding effect, we calculate the electrostatic potential surface, and the results are shown in Fig. 2. The regions of the negative electrostatic potential (denoted by red) are usually used to identify the hydrogen bonding acceptor sites. On the contrary, to describe the hydrogen bonding donating moieties, the regions of positive potential (denoted by bluish) are prominent. It can be clearly found that the negative electrostatic potentials for O_1 and O_4 atoms lead the intramolecular dual hydrogen bonds O_1–$H_2\cdots N_3$ and O_4–$H_5\cdots N_6$ to form for 1-enol. To further reveal the intramolecular interactions in the real space, we also calculate the reduced density gradient (RDG) and the $\mathrm{sign}(\lambda_2)\rho$ since they are a pair of very important functions for exploring weak interactions by using the NCI method. The corresponding results are shown in Fig. 3. The lower panel shows the low-gradient isosurface for 1-enol. Obviously, the spikes located in the dashed rectangular frame correspond to the hydrogen bonding interactions in the ground state. Moreover, we also consider the non-hydrogen bonding 1-open form, since the non-hydrogen bonding form can serve as a kind of comparison. In our calculation results, the bond length O_1–H_2 and O_4–H_5 for 1-open form are both 0.9663 Å in the ground state, whereas they become 0.9869 Å for 1-enol configuration. It further confirms the formation of dual hydrogen bonds O_1–$H_2\cdots N_3$ and O_4–$H_5\cdots N_6$ for 1-enol in the S_0 state.

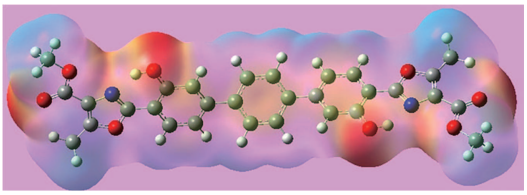


Fig. 2. Total electron density isosurface map with molecular electronic potential (MEP) for 1-enol structure, where values are selected from negative (red) to positive (blue): −0.05 a.u.–0.05 a.u.

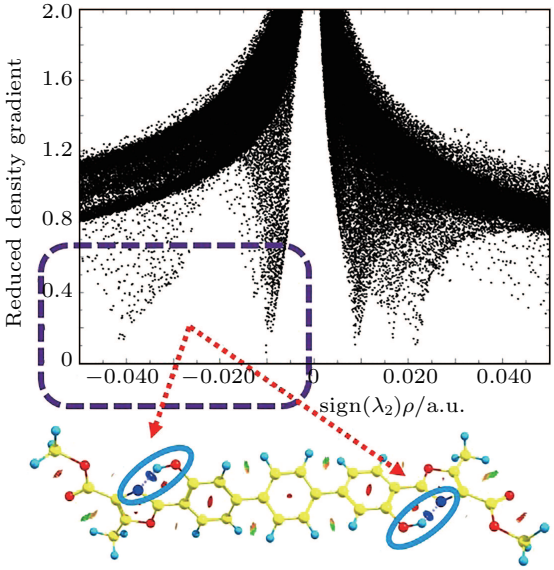


Fig. 3. RDG *versus* $\mathrm{sign}(\lambda_2)\rho$ as well as low-gradient ($s = 0.50$ a.u.) isosurface (lower panel) for ground-state 1-enol system. Interactions can be seen below corresponding RDG (red: steric effect; blue: hydrogen bonding effect; green: VDW effect.).

The most important geometrical parameters (*i.e.*, bond lengths and bond angles) involved in hydrogen bonding moieties for 1-enol, 1-spt, and 1-dpt forms are listed in Table 1. It is obvious that the 1-enol configuration is symmetrical, and the bond lengths and bond angles of symmetrical parts are equivalent. Specifically speaking, the lengths of O_1–H_2 and O_4–H_5 bond of 1-enol in the ground state are both 0.9869 Å and elongated to 0.9971 Å in the first excited state. While for hydrogen bonds $H_2\cdots N_3$ and $H_5\cdots N_6$ for 1-enol structure, it can be found that they are shortened from S_0-state 1.8159 Å to S_1-state 1.7924 Å. Meanwhile, the bond angles $\Delta(O_1$–$H_2\cdots N_3)$ and $\Delta(O_4$–$H_5\cdots N_6)$ are also increased slightly from 145.9° to 148.5° in the first excited state. All these changes of geometrical parameters demonstrate that the dual intramolecular hydrogen bonds O_1–$H_2\cdots N_3$ and O_4–$H_5\cdots N_6$ of 1-enol are strengthened in the S_1 states.[11–16] In fact, even though the amplitude of variations is not very large, they are enough to affect the excited state dynamical behaviors for chemical systems.[57–62] For the case of excited state hydrogen bonding interactions and relative dynamics, it has to be mentioned that infrared (IR) vibrational spectrum is a very important manner to explore and compare the similarities and differences of hydrogen bonds between S_0 and S_1 states.[11–16,57–62] Therefore, in this work, we also perform the quantum chemical simulations about IR vibrational spectra by referring to the hydrogen bonding moieties. As shown in Fig. 4, the conjunct vibrational region of O_1–H_2 and O_4–H_5 stretching vibrational modes for 1-enol in S_0 and S_1 states are displayed. One can find that the theoretical O_1–H_2 and O_4–H_5 stretching modes are both located at 3252 cm^{-1} in the S_0 state, while they are downshifted by 86 cm^{-1} from 3252 cm^{-1} to 3166 cm^{-1} in the S_1 state. It further confirms that the dual intramolecular hydrogen bonds O_1–$H_2\cdots N_3$ and O_4–$H_5\cdots N_6$ should be strengthened in the S_1 state.[11–16,57–62]

Table 1. Simulated bond distances (in unit Å) and bond angles (°) involved in hydrogen bonding moieties for 1-enol, 1-spt, and 1-dpt forms in both S_0 and S_1 states based on the DFT/TDDFT method in DMSO solvent, respectively.

	1-enol		1-spt		1-dpt	
	S_0	S_1	S_0	S_1	S_0	S_1
O_1–H_2	0.9869	0.9971	1.7739	2.0191	1.7723	1.8012
H_2–N_3	1.8159	1.7924	1.0361	1.0189	1.0364	1.0321
O_4–H_5	0.9869	0.9971	0.9870	0.9878	1.7723	1.8012
H_5–N_6	1.8159	1.7924	1.7946	1.7943	1.0364	1.0321
Δ(O_1–H_2–N_3)	145.9°	148.5°	130.3°	120.9°	130.3°	128.4°
Δ(O_4–H_5–N_6)	145.9°	148.5°	145.9°	146.6°	130.3°	128.4°

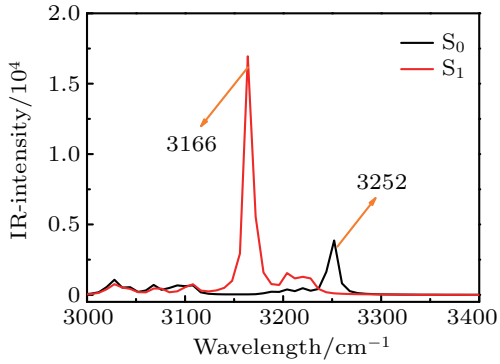


Fig. 4. Our theoretical IR spectrum of O_1–H_2 and O_4–H_5 stretching vibrational modes for 1-enol structure in S_0 and S_1 states based on DFT and TDDFT methods, respectively.

Furthermore, it cannot be denied that hydrogen bonding energy should be a more effective and visual physical quantity to check the variation between S_0 and S_1 states. Therefore, we also calculate the hydrogen bonding energy in S_0 and S_1 states for 1-enol system. Hydrogen bonding energy is calculated by subtracting the energy of 1-open configuration from the energy of 1-enol structure. In fact, it is imperative to emphasize at this stage that the estimation of the intramolecular hydrogen bonding energy according to the energy difference between the 1-enol and 1-open configurations produced by the rotation of the twist angle supports the assumption of no other geometry effects as a result of the rotation for hydroxyl O–H. Even though the assumption is perhaps inadequate for simulating the intramolecular hydrogen bonding energy, previous work has proved the feasibility of this method for comparing bonding energy approximately.[62–64] The simulated hydrogen bonding energy of 1-enol in the S_0 state is about 8.35 kcal/mol, while that of 1-enol in the S_1 state is 12.17 kcal/mol. Thus, we can confirm that the hydrogen bonding does strengthen in the first excited state, which provides the possibility for the ESIPT process.

Table 2. Theoretical electronic excitation energy (λ nm), corresponding oscillator strengths (f) and corresponding compositions of 1-enol configuration in DMSO solvent for three different transtions.

Transitions	λ/nm	f	Composition	Percentage/%
$S_0 \rightarrow S_1$	339	1.9635	H → L	98.93
$S_0 \rightarrow S_2$	303	0.0105	H-2 → L	82.25
$S_0 \rightarrow S_3$	286	0.0035	H → L+1	77.26

To examine the effects originating from photo-excitation process, the vertical excitation process from the S_0-state optimized 1-enol configuration is also calculated by using TDDFT with the six low-lying absorbing transitions in DMSO solvent. For convenience, the simulated electronic transition energy values, relative oscillator strengths and compositions of first three transitions are listed in Table 2. It can be found clearly that the absorption peak of the first transition ($S_0 \rightarrow S_1$) is calculated to be at 339 nm, which is in good agreement with the experimental result (332 nm).[36] At least, it can be confirmed that the TDDFT/B3LYP/TZVP theoretical level is enough to describe the 1-enol system. In addition, to qualitatively discuss the change of charge redistribution in the photo-excitation process, the theoretical frontier molecular orbitals (MOs) of 1-enol are also simulated, and displayed to further elaborate the properties of electronic excited states (Fig. 5). It is clear that the first excited state mainly has the $\pi\pi^*$-type-character with the transition from the highest occupied molecular orbital (HOMO) to the lowest unoccupied molecular orbital (LUMO). From Table 2, it should be noticed that the HOMO–LUMO transition possesses a very large oscillator strength (1.9635), which means the evident absorption in previous experiment.[36] Here, we just show the HOMO and LUMO orbitals in the present work, since this transition almost includes the entire percentage (*i.e.*, 98.93%). That is to say, the transition from HOMO to LUMO can be adopted to describe the excited state property of the transition $S_0 \rightarrow S_1$. The higher transitions (*i.e.*, $S_0 \rightarrow S_2$, $S_0 \rightarrow S_3$ or others) are not considered in this work, since the oscillator strengths of them are too low. Particularly, the $S_0 \rightarrow S_3$ and higher transitions should be in the dark states. For the HOMO–LUMO transition, one thing should be noted that different parts could be located in range from HOMO to LUMO. Here, we mainly pay attention to the shifted moieties involved in the dual intramolecular hydrogen bonds (O_1–$H_2 \cdots N_3$ and O_4–$H_5 \cdots N_6$). Although none of the variations in O_1–H_2 and O_4–H_5, and N_3 and N_6 is very apparent, the quantitative proportions of the occupation are obviously different. The contribution proportions of O_1 and O_4, and N_3 and N_6 on the HOMO are around 4.27% and 3.98% for 1-enol, while their corresponding contribution proportions of the same atoms change to around 2.54% and 5.15% on the

LUMO orbital. That is to say, after the excitation, the driving force could be induced via increasing electronic densities around proton acceptors N_3 and N_6 moieties, which facilitates the proton transfer reaction for 1-enol system in the first excited state.

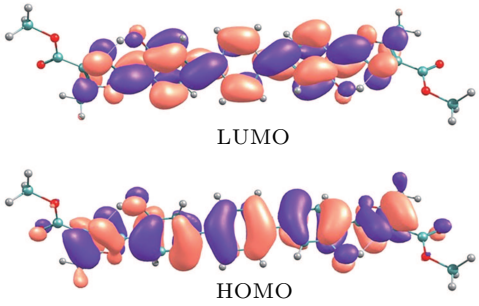


Fig. 5. Corresponding frontier molecular orbitals (HOMO and LUMO) for 1-enol system based on TDDFT/B3LYP theoretical level.

Even though the tendency of ESIPT can be revealed via the above-mentioned analyses, the detailed mechanism is lacking. In fact, the double ESIPT process mentioned is questionable since the energy of the stable 1-dpt form in the first excited state is higher than that of the 1-spt form although the solvent was not considered in Ref. [36]. Therefore, in this part, we mainly focus on the detailed ESIPT mechanism for 1-enol system. Based on DFT//TDDFT/B3LYP/TZVP level in DMSO solvent, we construct potential energy surfaces (PESs) for 1-enol system in S_0 state and S_1 state, with O_1–H_2 and O_4–H_5 bond lengths fixed. Here, we should mention that although previous work has reported that the TDDFT theoretical level cannot be provide the sufficiently accurate ordering of closely space excited states, theoretical results have shown the reliability of this method to offer qualitative energetic pathways for ESIPT behaviors.[41–49] Specifically, the constructed PESs of S_0 and S_1 states are realized through fixing O_1–H_2 and O_4–H_5 ranging from 0.9 Å to 2.1 Å in steps of 0.1 Å (see Fig. 6). As shown in Fig. 6(a), it can be clearly seen that the potential energy increases with the elongation of O_1–H_2 and O_4–H_5 bond lengths. That is to say, the forward proton transfer process cannot occur in the ground state for 1-enol system. While in the S_1 state, it is obvious that the optimized S_1-state 1-dpt form is the most unstable one with the highest potential energy. In other words, it is difficult for the excited state intramolecular double proton transfer to occur in the 1-enol system. Since the potential energy barrier is the best evidence to judge whether the excited state double proton transfer occurs. In addition, we further calculate the potential energy barriers. Because the synergetic double proton transfer occurs from 1-enol to 1-dpt along the diagonal line of Fig. 6(b), we find that high potential energy barrier is about 9.318 kcal/mol. While from 1-enol to 1-spt, the forward potential energy barrier is low (2.075 kcal/mol). It means that the excited state intramolecular single proton transfer pathway is easier than the synergetic double proton transfer way. In addition, we also consider the stepwise double proton transfer case. The potential energy barrier from 1-spt to 1-dpt is calculated to be 6.497 kcal/mol, while the reversed potential barrier (*i.e.*, from 1-dpt to 1-stp) is 1.924 kcal/mol. That is to say, even if the second step proton transfer occurs from 1-spt to 1-dpt, most of the 1-dpt species can return to the 1-spt one. Therefore, we can confirm that only the excited state single proton transfer occurs in the 1-enol system although it possesses two intramolecular hydrogen bonds.

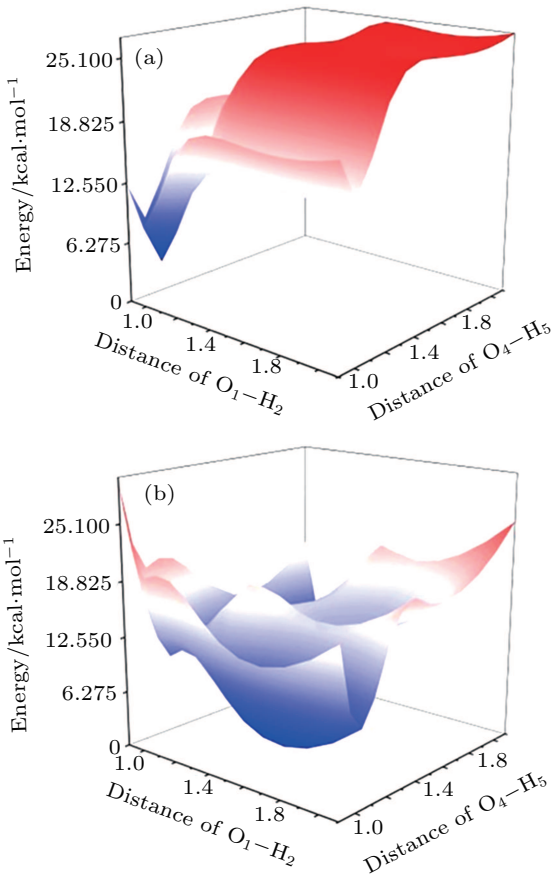


Fig. 6. constructed potential energy profile for S_0 and S_1 states for 1-enol system, with O_1–H_2 and O_4–H_5 bond distances fixed, obtained by DFT and TDDFT methods, respectively.

4. Conclusions

In this work, we theoretically explore the excited state intramolecular double hydrogen bonding interactions and ESIPT behaviors for the novel 1-enol system. Comparing the geometrical parameters and corresponding IR spectra of hydrogen bonding moieties of 1-enol in both S_0 and S_1 states, we verify the strengthening of dual intramolecular hydrogen bonds for 1-enol in the first excited state. After investigating the charge distribution and charge transfer resulting from photo-excitation process, we present that the increased electronic densities around proton acceptors play an important role in attracting hydrogen proton. That is to say, the driving force for ESIPT process can be produced by charge redistribution.

Further, we construct the PESs of both S_0 and S_1 states each with an ESIPT pathway. Based on the PESs, we confirm the excited state intramolecular single proton transfer mechanism for 1-enol system. Our work could let researchers have an in-depth understanding of the excited state behaviors involved in multiple hydrogen bonding interactions, and also figure out the detailed ESIPT mechanism for the novel 1-enol system. We expect that this work could play a role in paving the way for revealing and developing novel applications based on 1-enol molecule in future.

References

[1] Olsen S and Smith S 2008 *J. Am. Chem. Soc.* **130** 8677
[2] Wu Y, Han W, Wang D, Gao Y and Zhao Y 2008 *Acc. Chem. Res.* **41** 1418
[3] Tung C, Wu L, Zhang L and Chen B 2003 *Acc. Chem. Res.* **36** 39
[4] Zhao J, Dong H, Yang H and Zheng Y 2018 *Org. Chem. Front.* **5** 2710
[5] Demchenko A, Tang K and Chou P 2013 *Chem. Soc. Rev.* **42** 1379
[6] Liu Y, Mehata M and Liu J 2011 *J. Phys. Chem. A* **115** 19
[7] Liu Y, Wang S, Zhu C and Lin S 2017 *New J. Chem.* **41** 8437
[8] Zhao H, Sun C, Liu X, Yin H and Shi Y 2019 *Chin. Phys. B* **28** 018201
[9] Zhao H, Yin H, Liu X, Li H, Shi Y, Liu C, Jin M, Gao J, Luo Y and Ding D 2019 *J. Phys. Chem. Lett.* **10** 3064
[10] Weller A 1955 *Naturwissenschafter.* **42** 175
[11] Zhao G and Han K 2008 *Biophys. J.* **94** 38
[12] Zhao G, Northrop B, Han K and Stang P 2010 *J. Phys. Chem. A* **114** 9007
[13] Zhao G and Han K 2009 *J. Phys. Chem. A* **113** 4788
[14] Zhao G and Han K 2012 *Acc. Chem. Res.* **45** 404
[15] Zhao G and Han K 2008 *J. Comput. Chem.* **29** 2010
[16] Zhao G and Han K 2010 *Phys. Chem. Chem. Phys.* **12** 8914
[17] Zhao J, Dong H, Yang H and Zheng Y 2019 *ACS Appl. Bio. Mater.* **2** 2060
[18] Du C, Zhou Q, Zhang M, Song P and Ma F 2019 *J. Phys. Org. Chem.* **32** e3901
[19] Li J, Zhang M, Guo Y, Zhao M, Song P and Li X 2019 *J. Chin. Chem. Soc.* **66** 385
[20] Huang J, Wu J, Dong H, Song P and Zhao J 2017 *Commun. Comput. Chem.* **5** 27
[21] Boonkipatarakul K, Wang J, Niamnont N Liu B, Mcdonald L, Pang Y and Sukwattanasinitt M 2016 *ACS Sens* **1** 144
[22] Abeywickrama C and Pang Y 2017 *Tetrahedron Lett.* **58** 1627
[23] Liu Y, Wang S, Wang C, Zhu C, Han K and Lin S 2016 *J. Chem. Phys.* **145** 164314
[24] Zhao J, Yao H, Liu J and Hoffmann M 2015 *J. Phys. Chem. A* **119** 681
[25] Wang J, Chen W, Liu X, Wesdemiotis C and Pang Y 2014 *J. Mater. Chem. B* **2** 3349
[26] Zhang T, Yang G, Jia M, Song X, Zhang Q and Yang D 2018 *J. Phys. Org. Chem.* **31** e3857
[27] Chen Y, Wu P, Peng C, Shen J, Tsai C, Hu W and Chou P 2017 *Phys. Chem. Chem. Phys.* **19** 28641
[28] Liu Y, Lan S, Zhu C and Lin S 2015 *J. Phys. Chem. A* **119** 6269
[29] Zhao J, Chen J, Liu J and Hoffmann M 2015 *Phys. Chem. Chem. Phys.* **17** 11990
[30] Tang K, Chen C, Chuang H, Chen J, Chen Y, Lin Y, Shen J, Hu W and Chou P 2011 *J. Phys. Chem. Lett.* **2** 3063
[31] Zhao J, Chen J, Cui Y, Wang J, Xia L, Dai Y, Song P and Ma F 2015 *Phys. Chem. Chem. Phys.* **17** 1142
[32] Zhao J, Dong H and Zheng Y 2018 *J. Phys. Chem. A* **122** 1200
[33] Zhao J, Dong H and Zheng Y 2018 *J. Lumin.* **195** 228
[34] Liu Y, Lan S and Li C 2013 *Spectrochim. Acta Part. A* **112** 257
[35] Zhang Z, Chen Y, Hung W, Tang W, Hsu Y, Chen C, Meng F and Chou P 2016 *Chem. Mater.* **28** 8815
[36] Reis J, Fernandes A, Freitas-Dorr B, Bastors E and Stefani H 2018 *Tetrahedron* **74** 6866
[37] Cong L, Yin H, Shi Y, Jin M and Ding D 2015 *RSC Adv.* **5** 1205
[38] Yin H and Shi Y 2018 *Chin. Phys. B* **27** 058201
[39] Zhao Y, Wang M, Zhou P, Yang C, Ma X, Tang Z and Bao D 2018 *J. Phys. Org. Chem.* **31** e3803
[40] Li H, Shi Y, Yin H, Wang Y, Cong L, Jin M and Ding D 2015 *Spectrochim. Acta Part. A Mol. Biomol. Spectrosc.* **141** 211
[41] Liu S, Ma Y, Yang Y, Liu S, Li Y and Song Y 2018 *Chin. Phys. B* **27** 023103
[42] Zhou P and Han K 2018 *Acc. Chem. Res.* **51** 1681
[43] Li G, Song P and He G 2011 *Chin. J. Chem. Phys.* **27** 305
[44] Li G and Chu T 2011 *Phys. Chem. Chem. Phys.* **13** 20766
[45] Li G, Zhao G, Han K and He G 2011 *J. Comput. Chem.* **32** 668
[46] Li G, Zhao G, Liu Y, Han K and He G 2010 *J. Comput. Chem.* **31** 1759
[47] Tang K, Chang M, Lin T, Pan H, Fang T, Chen K, Hung W, Hsu Y and Chou P 2011 *J. Am. Chem. Soc.* **133** 17738
[48] Li G and Han K 2018 *WIREs Comput. Mol. Sci.* **8** e1351
[49] Frisch M, Trucks G, Schlegel H, *et al.* 2009 *Gaussian 09*, revision D.01; Gaussian, Inc., Wallingford, CT
[50] Lee C, Yang W and Parr R 1988 *Phys. Rev. B* **37** 785
[51] Becke A 1993 *J. Chem. Phys.* **98** 5648
[52] Miehlich B, Savin A, Stoll H and Preuss H 1989 *Chem. Phys. Lett.* **157** 200
[53] Feller D 1996 *J. Comput. Chem.* **17** 1571
[54] Cammi R and Tomasi J 1995 *J. Comput. Chem.* **16** 1449
[55] Cances E, Mennucci B and Tomasi J 1997 *J. Chem. Phys.* **107** 3032
[56] Li J, Zhang M, Du C, Song P and Li X 2018 *J. Phys. Org. Chem.* **31** e3867
[57] Han J, Liu X, Li H, Yin H, Zhao H, Ma L, Song Y and Shi Y 2018 *Phys. Chem. Chem. Phys.* **20** 26259
[58] Li J, Li X, Cheng S, Song P and Zhao J 2018 *J. At. Mol. Sci.* **9** 1
[59] Yin H, Zhang Y, Zhao H, Yang G, Shi Y, Zhang S and Ding D 2018 *Dyes Pigm.* **159** 506
[60] Wei Q, Wang J, Zhao M, Zhang M, Song Y and Song P 2018 *Can. J. Chem.* **96** 83
[61] Li H, Yin H, Liu X, Shi Y, Jin M and Ding D 2017 *Spectrochim. Acta Part. A* **184** 270
[62] Maheshwari S, Chowdhury A, Sathyamurthy N, Mishra H, Tripathi H, Panda M and Chandrasekhar J 1999 *J. Phys. Chem. A* **103** 6257
[63] Mahanta S, Paul B, Singh R and Guchhait N 2011 *J. Comput. Chem.* **32** 1
[64] Paul B and Guchhait N 2012 *J. Lumin.* **132** 2194